The ink metering process with two counterrotating rollers - simulation and experiment

Martin Berg, Dipl.-Ing. M.Sc.*

Keywords: Ink Flow, simulation, testing

Abstract

A two roller inking unit is presented. The ink is separated, accelarated and metered at one single nip. The focus is put on the simulation of the metering process and on its experimental verification.
A finite-element analysis (FEA) is applied to simulate the ink flow. The rollers are modelled as rigid rollers, counterrotating with various speed differentials. The material properties of the ink are characterised by the density, the surface tension and the viscosity. Here the power-law modell is applied to express the viscosity. The used values are taken form measurements with a conventional sheetfed offset ink.
The simulations deliver a inverse dependance of the metered inkfilm thickness ratio from the roller's speed ratio. These results could be verified with experimental data retrieved from a self designed metering device.
Further aspects of the FEA, especially concerning the surface tension, are dicussed as well as the quality of the metered ink film (smoothness, ribbing). Methods of introducing a rubber roller in the simulation are offered.
All in all it is shown that commercial software applying FEA can be used to predict the metering behaviour of the two-roller- unit and that it can be incorporated into the design process of a inking unit.

* Oce´ Printing Systems GmbH, Germany

Nomenclature

symbol	*unit*	*description*
b	µm	Inkfilm thickness on paper
k	$Pa \cdot s^n$	parameter of the Ostwald model
l_0	m	arclength along the free surface
n	-	parameter of the Ostwald model
p	Pa	pressure
q	N/mm	line pressure
r	mm	radius
s	µm	film thickness
h	µm	gap width
T_0	mN/m	surface tension
u	m/s	velocity

Greek letters		
$\dot{\gamma}$	1/s	shear rate
κ	s	parameter of the Carreau model
τ	Pa	shear stress
η	Pa·s	viscosity
ρ	g/cm^3	density

Subscripts	
1	roller 1
2	roller 2
m	mean

1. Introduction

Ink metering represents a difficult task in offset printing. Roller-type inking units have long reaction times and cause increased paperwaste for the setup. Anilox and injection inking units require optimized inks. The design is relatively complex. A two roller inking unit with two counterrotating rollers and a reservoir in between offers the opportunity to combine short reaction cycles, a simple design and the usage of standard offset inks. However, the metered ink film thickness have to be predictable. The study presents a simulation method of the ink metering process and compares the results with experiments on a selfdesigned two roller inking system.

2. Ink flow modelling

Several studies dealt with the flow in the nip of two counterrotating roller. They can be divided into a strictly phenomenological approach, a one-dimensional analytical approach and finite-element analysis (FEA). Also the modelled rollers can be a pair of rigid roller or a pair of a rigid and a deformable roller. The latter roller pair is not investigated in this paper.

Phenomenological models postulate equations using different weighting factors which are derived from experiments. No derivation from a basic law of physics is given. Several parameters are incorporated into the model e.g. temperature, absolute roller speed and the percentage of fountain solution within the ink-fountain emulsion. All these models are derivations of the equation (1) establis-

hed by Walker and Fetsko (1955) where b is the acceptance capacity of stock surface for ink.

$$s_{Print} = b + f\left(s_{Plate} - b\right) \tag{1}$$

These models assume two incoming inkfilms of a defined thickness and ignore the possibility of speed differences between the rollers. For that reason and the lacking desciption of ink properties they can be discarded for the ink metering out of a reservoir.
Other studies describe the pressure and pressure gradient based on a one-dimensional analytical approach (Ritz and Rech, Savage). Savage (1982) further derives a relation of the ink film ratio after the separation depending on the speed ratio of the rollers.

$$\frac{s_2^{\infty}}{s_1^{\infty}} = \alpha\left(\frac{u_2}{u_1}\right)^{\beta} \tag{2}$$

Savage determines the parameters α with 1 and β with 0,5 for flows without cavitation. However, a one-dimensional pressure gradient can not be employed for the flow at the nip outflow, because the flow becomes two-dimensional.

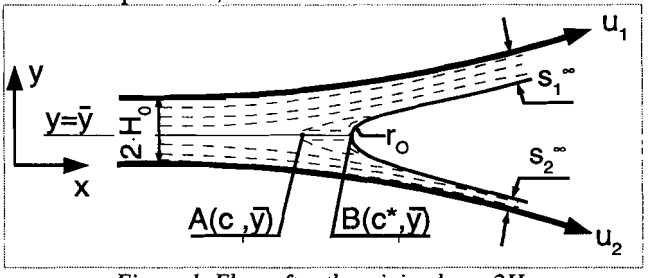

Figure 1. Flow after the minimal gap $2H_0$

A finite-element analysis (FEA) can model a two-dimensional flow. It also allows to calculate the location of the free boundary at the outflow meniscus. Several studies have applied a FEA (Benjamin et al., 1994; Coyle et al., 1982). The limitations of these studies consist in the use of a newtonian fluid or waterlike Reynolds-Numbers Re and Capillarity-Numbers Ca.

$$Re = \frac{H_0 \cdot u \cdot \rho}{\eta} \tag{3}$$

$$Ca = \frac{\eta \cdot u}{T_O} \tag{4}$$

The viscosity of an average offset ink is about three magnitudes larger than those of water. Thus the Reynolds-Number of offset ink is at similar speed and gap width about thousand time smaller and the Capillary-Number is about thousand times lager. The flow pattern changes, e.g. small laminar eddies at the outflow meniscus disappear. Effects caused by the shear-thinnig behaviour of offset inks

can be expected. For that reasons the FEA was based on the model of Benjamin et al., but some extensions were added.
The flow modelling includes the following assumptions:

- two parallel and rigid roller of infinite width
- a floated gap entrance
- no flow in axial roller direction
- steady, isothermal and incompressbile flow
- ideal adhesion of the inks on the roller surface

This results in a simplified Navier-Stokes equation (5) and a simplified continuity equation (6).

$$\rho(\mathbf{u}\cdot\nabla)\mathbf{u} = \rho\mathbf{g} - \nabla p + \eta\cdot\Delta\mathbf{u} \quad (5) \qquad \nabla\cdot\mathbf{u} = 0 \quad (6)$$

The free surface is characterized by the vanishing of the flow normal to the interface and the balance of normal stress $\mathbf{n}\cdot\mathbf{T}$ with the capillary pressure.

$$\mathbf{n}\cdot\mathbf{u} = 0 \quad (7) \qquad \mathbf{n}\cdot\mathbf{T} = \frac{1}{Ca}\frac{dt}{dl_o} - \mathbf{n}p_{atm} \quad (8)$$

In contrast to Benjamin et al. no velocity profile is given at the inflow boundary. However, the inflow boundary must be located far enough upstream to guarantee a fully developed flow before the smallest gap. The outflow flow boundaries are located further downstream where the viscous stress vanishes. Figure 2 shows a defining sketch of the flow domain.

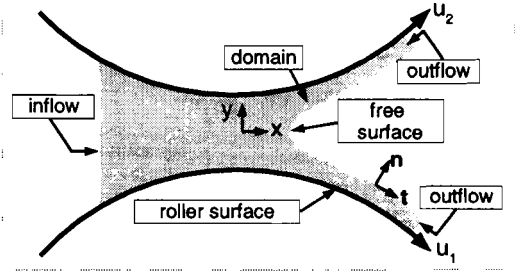

Figure 2. Flow domain and boundaries of the FEA

An estimation of the conditions in a ink metering gap provide Reynolds-Numbers smaller than 1. This creates a laminar flow and allow therefore a laminar modelling. The experimental determination of the surface tension of offset ink has not been reported yet. Since it is smaller than those of water (ca.72 mN/m) a value of 30 mN/m was assumed. Therefore the flow will be dominated by viscous forces. The influence of gravity is neglectable as well as the influence of inertia.
The analysis was performed using the commercial Software FIDAP. It runs on a Unix Workstation. Quadrangular elements were used for the simulations and at

the free surface the mesh was refined. The geometrical proportions of roller radius and gap width are fixed after the creation of the mesh. The material parameters and the roller speed can be changed afterwards. The parameters are defined in a nondimensionalzed form.
The calculation is executed in three steps where the solution from the previous step is applied as starting solution for the next step. First the free surface is fixed at the starting estimation to calculate a velocity field. Then the free surface is released. The calculation is carried out in a transient mode. This increases the tolerance between the starting solution and a possible converged solution–the convergence radius. Finally a steady calculation follows.

$$\eta(\dot{\gamma}) = \eta_\infty + \frac{(\eta_0 - \eta_\infty)}{\left(1 + (\kappa \cdot \dot{\gamma})^2\right)^{\frac{n-1}{2}}} \quad (9) \qquad \tau = k \cdot \dot{\gamma}^n \quad (10)$$

The software allows the incorporation of various non-newtonian viscosity models. The model most suitable to describe the viscosity-shear-behaviour of offset ink is the Carreau-Model, (9). It contains a starting viscosity η_0 for a zero shear rate, shear thinning region and an endviscosity η_∞. Results from measurements in a rotation viscosimeter with serveral offset inks can be good fitted with the model, see Figure 3. The Power-Law-Model by Ostwald, (10), simplifies the shear-thinning behaviour and is therefore better suited to visualize different intensities of shear-thinning. Table 1 shows the parameters of the inks used for the simulation and the experiments. The parameter result from regression calculations.

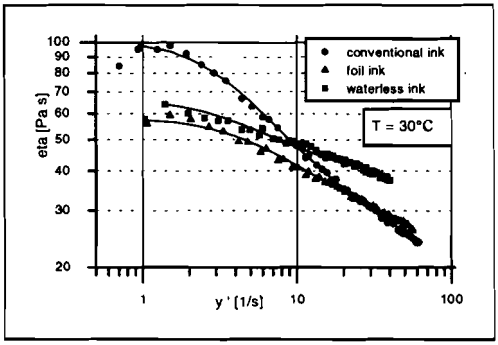

Figure 3. Viscosity vs. Shear rate plots and Carreau fitting curves for offset inks

Ink	*Ostwald Model*		*Carreau Model*			
	k	n	η_0	η_∞	κ	n
conventional ink	97,3	0,65	101,7	16,4	0,36	1,76
foil ink	67,6	0,76	58,1	12,5	0,26	1,44
waterless ink	73,1	0,82	65,9	33,5	0,31	1,71

Table 1: Parameter of different offset inks at 30°C

3. Simulation Results

The calculations were performed for the following array of parameters:

roller speed u_1	1, 2, 5, 10 m/s
speed ratio u_2/u_1	1 ... 0,25
minimal gap width $2H_0$	10, 20, 40 µm
roller radius r_1, r_2	90 mm
offset inks	foil ink, waterless ink, conventional ink

Foil ink was used for the calculations if not otherwise stated. Different viscosity models were only applied to foil ink. The material parameters were taken from the above mentioned measurements at 30°C which is a typical operation temperature in offset presses. The roller radius of 90 mm refers to the two-roller inking unit used for the experimental verifications.

All calculated parameter combinations yield flows without laminar eddies. A typical pressure distribution results with a positive pressure region in front of the minimal gap and a negative pressure region behind the minimal gap, Figure 4, always relative to atmospheric pressure.

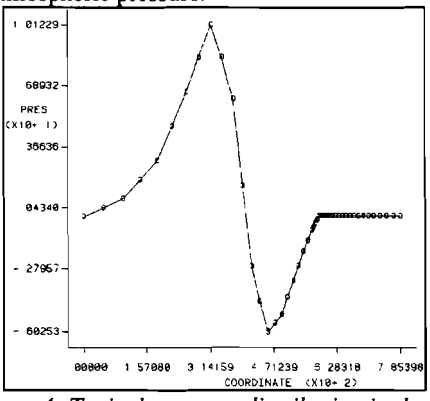

Figure 4: Typical pressure distribution in the nip

The absolute value of the pressure depends on the average roller speed $u_m=(u_1+u_2)/2$, the half gap width H_0 and the endviscosity η_∞. The same is true for the line pressure q - the integration of the pressure of the lenght of the nip. The following dependancies could be determined:

$$p \sim u_m \qquad p \sim \eta_\infty \qquad p \sim H_0^{-1,52} \qquad q \sim u_m \qquad q \sim \eta_\infty \qquad q \sim H_0^{-1,2}$$

The inflow boundary has to be located approximately 100 times the minimal gap width or further upstream of the minimal gap to eliminate the influence of varying inlet locations on the pressure distribution.

A speed distribution with a stagnation point (u=0) is calculated at the free surface independently from the roller speed ratio, see Figure 5.

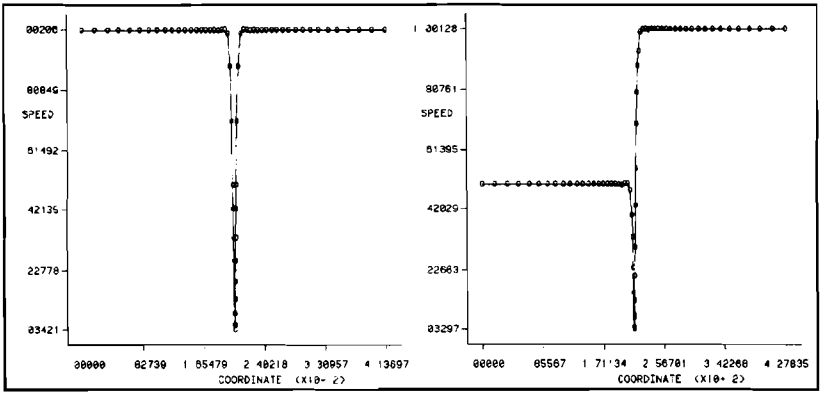

Figure 5: Speed distribution at the free surface - left $u_2/u_1=1$, right $u_2/u_1=0,5$

The maximal flow speed occurs always at the minimal gap and has the value of $1,41 \cdot u_1$ for equal roller speeds. The inkfilm thickness on both rollers is at equal speeds calcultated to $1,28 \cdot H_0$. These results are independent from the absolut values of speed and gap width. Variations amount to less than 1 percent.
The ink metering behaviour at varying speed differences is described according to equation (2) with the parameter α and β. α represents the symmetry of metering at equal speeds. Since two identical rollers are modelled α was like expected always 1 with very slight variations. β expresses the influence of an asymmetric speed ratio u_2/u_1 on the inkfilm thickness ratio s_2/s_1. A regression calculation delivered α and β basing on a set of simulations at different speed ratios but constant gap width or constant absolute speed of roller 1.

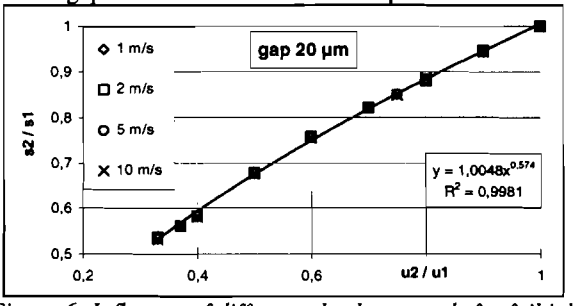

Figure 6: Influence of different absolute speeds for foil ink

The absolute speed does not influence the metering behaviour. β remains constant at 0,57 as Figure 6 shows at the given gap width. A changing gap width effects the the metering behaviour slightly, see Figure 7.
The three inks, although with considerable differences in their shear rate - shear stress function, do not show varying metering behaviour, Figure 8. This brings up the question if the shear thinning behaviour influences the metering and the

resulting inkfilm thicknesses at all. Therefore the viscosity distribution close to the stagnation point at the free surface is investigated.
The ink viscosity increases after the minimal gap and reaches shortly after the stagnation point its starting value η_0, see Figure 9. The enlaged meniscus in Figure 10 shows that the region with a viscosity higher than endviscosity is situated directly at the dividing streamline.

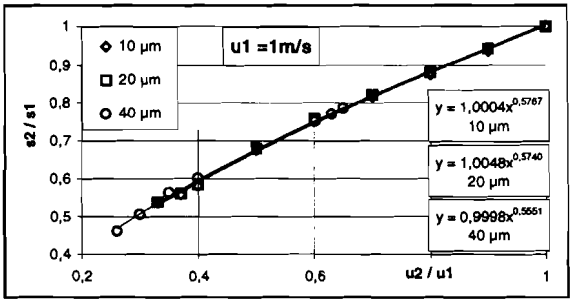

Figure 7: Influence of different absolute gap widths for foil ink

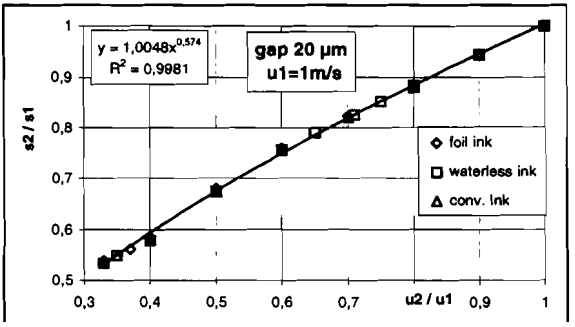

Figure 8: Influence of different offset inks

Figure 9: Viscosity differences along the nip
(u_2/u_1=0,33; $2H_0$=40µm), (black-17,5 Pa·s; lightgray-12,5 Pa·s=η_∞)

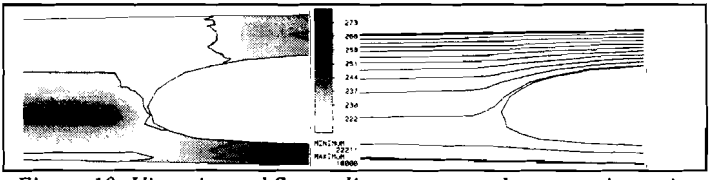

Figure 10: Viscosity and Streamline pattern at the stagnation point
(u_2/u_1=0,33; $2H_0$=40µm), (black-17,5 Pa·s; lightgray-12,5 Pa·s=η_∞)

For a better simulation of different shear-thinning behaviour the Ostwald viscosisty model is introduced. The power n determines the amount of shear thinning. A newtonian liquid is characterized by n = 1.
First a comparison between results of calculations applying the Carreau model and the Ostwald model for the foil ink was made. The Ostwald model produces a more asymetric film splitting, Figure 11. This can be explained by the lack of an endviscosity. The maximal shear rates calculated fall within the range of 0,79 to $0{,}89 \cdot (u_1/H_0)$. The total value of shear rates reaches 40000 to 1800000 1/s according to the observed range of gap widths and speeds. In any case the endviscosity of the Carreau model is reached. Variations fo the the paramter n in Figure 12 underline this discrepancy.

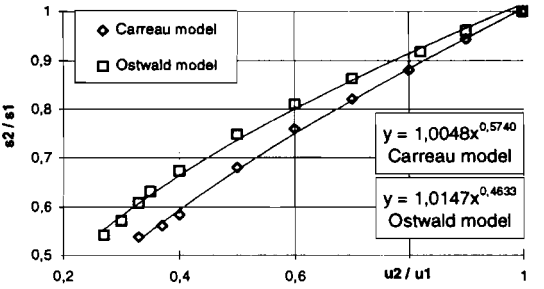

Figure 11: Influence of the viscosity model with foil ink ($2H_0$=20 μm, u_1=1 m/s)

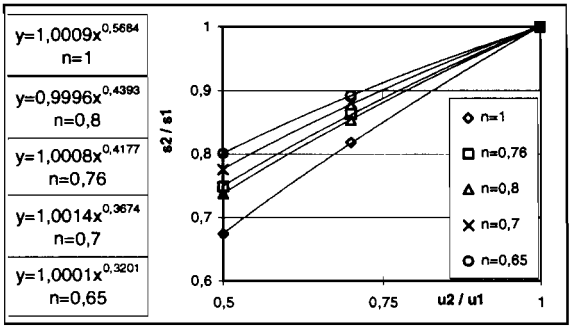

Figure 12: Influence of the shear-thinning parameter n of the Ostwald model

4. Experiments

An experimantal device was designed to verify the calculated results. It consists of two metall roller with a radius of 90 mm and a width of 300 mm. They were designed to omit bending caused by the hydrodynamic forces in the nip. Each roller is driven independently. The rollers are aligned horizontally so that the ink flow parallel to the direction of gravity.

During the experiment speed differences of 0,65 to $2,3 \cdot u_2/u_1$ were tested. The absolut speed varied between 1 m/s and 6,3 m/s. The gap width was adjusted to 10, 20, 30 and 40 µm. For the further analysis the results are ordered by the gap with. The regression calculation according equation (2) provides good correlations with correlation coefficents R^2 of 0,66 to 0,9. This proves the general suitability of the model used. α varies between 0,987 and 1,12, in other words an almost symmetrical splirring at equal speeds. β ranges from 0,54 at 40 µm up to 0,81 at 10 µm. The differences between the experimental results and the simulated ones can be explained by the existance of a roller surface roughness. It causes a boundary layer zone which becomes more important at smaller gap. The simulation does not incorporates the boundary layer zone. Therefore the correspondance of the β-values between simulation and experiment is good at larger gaps (30µm, 40µm). Differences increase with narrowing gaps. The experimental results are displayed in Figure 13, Figure 14, Figure 15 and Figure 16.

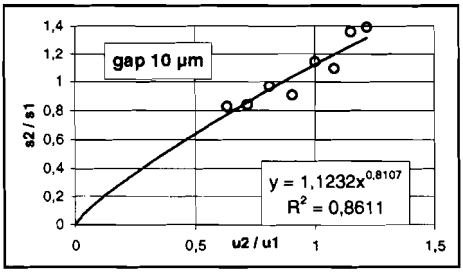

Figure 13: Film ration vs. Speed ration at a gap of 10 µm

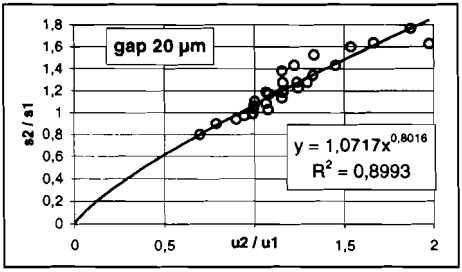

Figure 14: Film ration vs. Speed ration at a gap of 20 µm

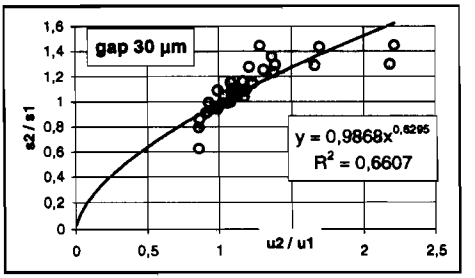

Figure 15: Film ration vs. Speed ration at a gap of 30 µm

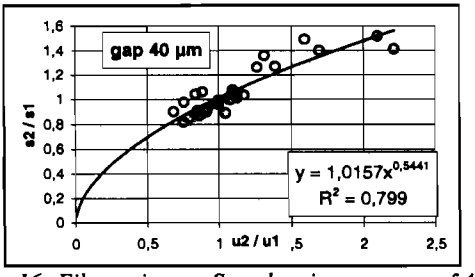

Figure 16: Film ration vs. Speed ration at a gap of 40 µm

The inkfilm thickness at equal speeds varied between 1,2 and 1,4·H_0. The variations result from deficiencies of the experimental device especially the presetting of the gap width or from the roughness of the metered ink films.
No sensor or measuring device was available to measure the pressure directly in the nip. The forces in the bearings were measured instead. This allows the calculation of the line pressure.

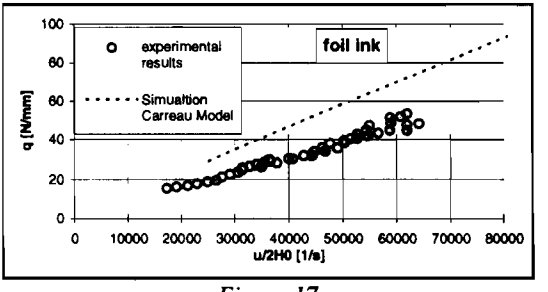

Figure 17

Figure 17 compares the measured and calculated line pressures. The measured values are about 4/5th of the calculated ones which has several reasons. One reason consists in possible the temperature difference of the ink between the experiments and the simulation. The experiments were carried out at 25 °C room temperature. A temperature of 28°C was measured at the roller surface However,

the inks heats itself up because of the shear. This can happen locally at the nip and disappear within one roller revolution. A raising temperatur causes a decreasing viscosity and thus a decreasing line pressure.
Another reason of the discrepancies could be the determination of the parameters of the Carreau model. The measurement takes place in a rotation viscosimeter at very low shear rates of 100 1/s or less. The endviscosity is calculated based on this values. The shear rates in the nip are two to three magnitudes higher.
The FEA calculation yields a pressure distribution with a negative pressure region. There values are reached which should lead to the onset of cavitation. But the model does not incorporates that.

5. Conclusions

The presented calculation method allows the simulation of the metering behaviour of a nip between two counterrotating rigid rollers. The metering behaviour can be described with a power-law model $s_2/s_1=1\cdot(u_2/u_1)^{0,57}$. Experiments have verified this simulation. The influences of the surface roughness of the rollers has to be taken into account at gaps smaller than 30 µm. The absolute metered inkfilm thickness per roller at equals speed corresponds to ca. 0,65 times the minimal gap width. The absolute roller speed does not influence the absolute film thickness nor the thickness ratio s_2/s_1.
The differences between calculated and measured load have to be investigated closer. The simulation should incorporate isothermal effects and threshold for the subatmospheric pressure. The measurements could be refined with a sensor measuring directly at the roller surface.
Despite this deficiencies it can be summarized that high loads a generated using a two-roller inking unit. The design of the rollers and the bearings has to account of that.

6. References

Walker, W.; Fetsko, J.:
A Concept of Ink Transfer in Printing, TAGA Annual Conference, Boston, 1955

Ritz, A.; Rech, H.:
Bestimmung der rheologischen Größen von Druckfarben im Farbwerk einer Offsetmaschine, FOGRA-Forschungsbericht 5.200, Munich, 1978

Savage, M.D.:
Mathematical Models for Coating Processes, J.Fluid Mech., !982, Vol. 117

Benjamin, D.F.; Carvalho, M.S.; Anderson, T.J.; Scriven, L.E.:
Forward Roll Film-Splitting: Theory and Experiment; TAPPI Coating Conference Proceedings, 1994, pp. 109-123

Coyle, D.J.; Macosko, C.W.; Scriven, L.E.:
Computer Simulation of Nip Flow in Roll Coating, American Chemical Society, 1982, (Computer Applications in Applied Polymer Science)

7. Acknowledgements

The author thanks the colleagues of the Technical University of Chemnitz for helpful discussions, especially Prof. Ruder.